Investigation of the equilibrium and non-equilibrium models of heat and moisture transport in a wet porous building material

Mirosław Seredyński[*,1], *Michał* Wasik[1], *Piotr* Łapka[1], *Piotr* Furmański[1], *Łukasz* Cieślikiewicz[1], *Karol* Pietrak[1], *Michał* Kubiś[1], *Tomasz S.* Wiśniewski[1] and *Maciej* Jaworski[1]

[1]Institute of Heat Engineering, Faculty of Power and Aeronautical Engineering, Warsaw University of Technology, 21/25 Nowowiejska St., 00-665 Warsaw, Poland

Abstract. In the paper the equilibrium and non-equilibrium models of moisture transport across the wet building material are proposed and compared. The equilibrium condition between gaseous and liquid moisture phases in the first model is relaxed in the second one, where evaporation and condensation are driven by the difference between the actual moisture partial pressure and its saturation value. In both models moisture is assumed in the gaseous phase as well as continuous (funicular) and discontinuous (pendular) liquid phase. Moreover, the transport of moisture is tightly coupled with heat transfer, which is treated as the fully equilibrium process in both models. The proposed models are verified with numerical results available in literature, namely with temporal variation of temperature in selected location in the building material. Additionally, predicted with both models temporal changes of the moisture content in three selected points and the total moisture content are compared. Both models produced similar results.

Nomenclature

a_s	– pores area per unit volume of the porous medium
B	– universal gas constant
c, c_p	– specific heat, specific heat at constant pressure
C_{dry}	– water vapor resistance diffusion factor
d_{av}	– average pore diameter
D	– mass diffusion coefficient
D^T, D^W	– coefficients in transport equations
h	– specific enthalpy
h_m	– convective mass transfer coefficient
h_t	– convective heat transfer coefficient
h_{lv}	– mass transfer coefficient between vapor and water in the porous medium
$\mathbf{j}$	– mass flux
k	– thermal conductivity
K_l	– liquid water permeability
$\dot{m}_{lv}$	– intensity (mass flow rate per unit volume) of evaporation/condensation
M	– molecular mass
p, p_c	– pressure, capillary pressure
s	– liquid saturation
t	– time
T	– temperature
Y	– vapor mass fraction
W, W_{cap}	– volumetric moisture content, capillary moisture content
Δh_{vl}	– latent heat of evaporation
ε	– volume fraction
ρ	– density

Subscripts and superscripts

a	– dry air
amb	– ambient
ef	– effective
g	– moist air
l	– liquid water
p	– pores
ref	– reference
s	– solid material
sat	– saturation conditions
v	– water vapor
w	– wall
0	– initial

1 Introduction

Transport of moisture in building materials is an important issue related to drying of buildings. It involves concurrent multi-phase water transport in the multi-scale porous structure which is accompanied by heat transfer. Water can take the form of gaseous phase as well as continuous (funicular) and discontinuous (pendular) liquid phase.

Several approaches for modeling of combined heat and mass transfer in different porous materials can be found in literature. For example, Van Belleghem et al. [1, 2] developed a new two-equation model of drying process of moist building materials which accounted for presence of gaseous and liquid moisture. The energy and moisture conservation equations were formulated with

* Corresponding author: msered@itc.pw.edu.pl

two independent state (transported) variables, i.e., temperature and capillary pressure. The model might be applied to study vapor diffusion through porous materials and capillary moisture transfer. Earlier, the same team presented similar but simplified model of heat and moisture transfer in porous materials with temperature and relative mass fraction of water vapor in the air as transported variables [3, 4]. The model was only valid in the hygroscopic range (i.e., for relative humidity < 98%), where the moisture transfer by equivalent vapor diffusion was dominant and the liquid transfer had minor significance (no continuous water phase in the pore system). Moreover, no air transfer occurred. In the next paper Janetti et al. [5] presented also two-equation model of heat and moisture transfer in porous building materials. The model was similar to the one developed by Van Belleghem et al. [1, 2], but the transported variable for moisture was relative humidity. The model which included combined heat as well as air and moisture transfer through porous building material was presented by Belleudy et al. [6]. In that model moisture transfer consisted of three main phenomena: vapor diffusion, vapor advection by air flow and capillary suction. By disregarding natural convection, they simplified and decoupled the problem of air flow in the porous materials from hygrothermal field. This enabled the velocity field to be solved prior to the hygrothermal field. Moreover, heat and moisture transfer equations were formulated in terms of temperature and relative humidity as transported variables. Allam et al. [7] developed the model of the hygrothermal transfer in the clay brick which utilized the temperature and vapor partial pressure as driving potentials. Recently, the model of heat and moisture transfer in porous building materials which consisted of four equations, i.e., energy, liquid moisture, vapor and dry air balance equation, was presented in [8, 9]. In this model temperature, liquid moisture volume fraction as well as vapor and dry air densities were used as independent variables. In the case of hygroscopic porous textile or fibrous materials heat and moisture transfer models are formulated applying, e.g., the temperature, water vapor concentration in pores, moisture concentration in fibers and water content in the fibrous batting as independent variables [8]. These models account for moisture movement induced by the partial water vapor pressure, a supersaturation state in condensing region as well as the dynamic moisture absorption of fibrous materials and the movement of liquid condensate. In turn, in the hygro-thermal model of protective clothing subjected to the high radiative heat flux developed by Łapka et al. [9, 10] the governing equations for heat and moisture transfer were formulated using the temperature, volume fraction of bound water and vapor density. This model accounted for conductive and radiative heat transfer accompanied by the diffusion of the vapor through fabrics with its phase transition to or from the bound state in fibers of fabrics.

In this study two approaches for the coupled heat and moisture transfer are considered. In the first one, a simplified model is based on the assumption of the local thermal and inter-phase mass transfer equilibrium. It takes into account transfer of liquid water and energy in the porous brick. In the proposed model two independent variables are assumed, namely the total moisture content and temperature. Transfer of liquid is driven mainly by gradient of total water content, but also by gradients of temperature. The equilibrium related to mass transfer at the interphase boundary is relaxed in the second model. Transport equations are expressed in the form of a multi-domain formulation. It means, the moisture transfer equation is derived for each virtual phase and interphase transport processes are expressed as source terms, dependent also on the microstructure of the porous brick material. The mass transfer between phases caused by evaporation or condensation is driven by difference between the actual partial moisture pressure and its saturation value. However, the thermal equilibrium conditions between various phases of water and the brick material is assumed. In the non-equilibrium model independent variables are the vapor density, liquid volume fraction and temperature.

In the next sections of the paper two proposed models are presented together with boundary and initial conditions as well as closing relationships. Moreover, the analyzed case is described, and data required in simulations are given. Then proposed models are verified in the simplified way and the results predicted by both models are compared in several points of the computational domain.

2 Descriptions of models

2.1 General assumptions

The considered wet brick (i.e., the wet porous building material) was assumed to consist of three phases: the solid material, free liquid water (in funicular and pendular state) and moist air (mixture of vapor and dry air). Bound water at the surface of solid component was neglected. The sum of volume fractions of these three phases was equal to one (i.e., $\varepsilon_s+\varepsilon_l+\varepsilon_g = 1$). The volume fraction of the solid component was assumed to be constant, while the sum of water and moist air volume fractions was equal to the volume fraction of pores (i.e., $\varepsilon_p = \varepsilon_l+\varepsilon_g$). The amount of vapor in pores in the building material was changed due to the vapor diffusion and evaporation or condensation phenomena, while the amount of water changed due to water movement related to the capillary pressure gradient and evaporation or condensation phenomena as well. The thermal equilibrium between different components and phases in porous building material was assumed. Moreover, in the non-equilibrium model, heat transfer due to moisture movement (i.e., the diffusion and capillary transport) was neglected. The total pressure in the porous material, p, was constant and equal to 101325 Pa, which allowed for the simplification of the mathematical model and elimination of dry air balance equation [8, 9].

2.2 Equilibrium model

The equilibrium model of heat and moisture transfer in the porous building material consisted of the following

balance equations for the total volumetric moisture content and energy:

$$\frac{\partial W}{\partial t}+\nabla\cdot\begin{bmatrix}\left(D_v^T+D_l^T\right)\nabla T\\+\left(D_v^W+D_l^W\right)\nabla W\end{bmatrix}=0 \tag{1}$$

$$\begin{aligned}&\frac{\partial}{\partial t}\left[\left(\rho c\right)_{ef}T\right]+\\&+\begin{bmatrix}\left(D_v^T c_{p,v}+D_l^T c_l+D_a^T c_{p,a}\right)\nabla T\\+\left(D_v^W c_{p,v}+D_l^W c_l+D_a^W c_{p,a}\right)\nabla W\end{bmatrix}\cdot\nabla T=\\&=\nabla\cdot\left(k_{ef}\nabla T\right)-\dot m_{lv}\Delta h_{vl}\end{aligned} \tag{2}$$

where the respective coefficients were defined as follows:

$$\begin{aligned}&D_v^T=-D_a^T=-\frac{M_a M_v}{M_g BT}D_{v,ef}\frac{\partial p_v}{\partial T}\\&D_v^W=-D_a^W=-\frac{M_a M_v}{M_g BT}D_{v,ef}\frac{\partial p_v}{\partial W}\\&D_l^T=K_l\frac{\partial p_c}{\partial T}\\&D_l^W=K_l\frac{\partial p_c}{\partial W}\end{aligned} \tag{3}$$

The intensity of evaporation and condensation is calculated with formula:

$$\dot m_{lv}=dW_v/dt \tag{4}$$

2.3 Non-equilibrium model

The non-equilibrium model of heat and moisture transfer in porous building material was formulated for evaporation and condensation phenomena which had finite rates. Hence, the following separated balance equations for gaseous and liquid moisture as well as energy were assumed:

$$\frac{\partial}{\partial t}\left(\varepsilon_g\rho_v\right)=\nabla\cdot\left(D_{v,ef}\nabla\rho_v\right)+\dot m_{lv} \tag{5}$$

$$\frac{\partial}{\partial t}\left(\varepsilon_l\rho_l\right)=-\nabla\cdot\left(K_l\nabla p_c\right)-\dot m_{lv} \tag{6}$$

$$\frac{\partial}{\partial t}\left[\left(\rho c\right)_{ef}T\right]=\nabla\cdot\left(k_{ef}\nabla T\right)-\dot m_{lv}\Delta h_{lv} \tag{7}$$

where intensities of evaporation and condensation were given by the following formulae:

$$\dot m_{lv}=\begin{cases}h_{vl}a_s\dfrac{\varepsilon_l}{\varepsilon_p}\left(\rho_{v,sat}-\rho_v\right)-\text{for evaporation}\\h_{vl}a_s\left(\rho_{v,sat}-\rho_v\right)-\text{for condensation}\end{cases} \tag{8}$$

The mass flow rate per unit volume had positive value for evaporation, while negative one for condensation. The $\varepsilon_l/\varepsilon_p$ ratio denotes the part of the pores area (volume) occupied by liquid moisture.

3 Numerical implementation

3.1 Description of the studied case

Numerical simulations were carried out for the case of drying of the ceramic brick of the thickness, L, equal to 3 cm which was schematically presented in Fig. 1. Only its top wall was in the contact with drying medium (i.e., air). The other walls, i.e., bottom and side walls were adiabatic and impermeable for moisture. Therefore, heat and moisture transfer in the considered brick was approximated by the one-dimensional (1D) transfer process.

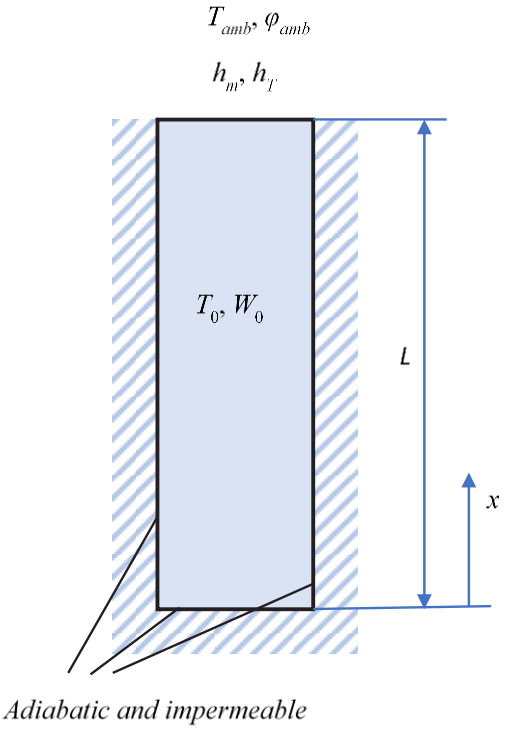

Fig. 1. Schematic of the considered computational domain with boundary and initial conditions.

The top wall of the brick was in the contact with flowing ambient air at temperature and relative humidity equal to T_{amb} and φ_{amb}, respectively. On this wall boundary conditions for eq. (1) and (2) were following:

$$\mathbf{j}_{v,w}+\mathbf{j}_{l,w}=h_m\left(\rho_{v,w}-\rho_{v,amb}\right) \tag{9}$$

$$\left(-k_{ef}\nabla T\right)_w+\mathbf{j}_{v,w}h_{v,w}+\mathbf{j}_{l,w}h_{l,w}=h_t\left(T_w-T_{amb}\right) \tag{10}$$

where mass fluxes and enthalpies were given by following formulae:

$$\mathbf{j}_v = D_v^T \nabla T + D_v^W \nabla W$$
$$\mathbf{j}_l = D_l^T \nabla T + D_l^W \nabla W \quad (11)$$

and

$$h_v = \Delta h_{vl} + c_{p,v}\left(T[K] - T_{ref}\right)$$
$$h_l = c_l\left(T[K] - T_{ref}\right) \quad (12)$$

On the same wall, boundary conditions for the non-equilibrium model, namely for eq. (5)-(7) were assumed to consist of two parts. For the first period of drying when liquid water in the pendular state was present at the boundary and evaporation from the surface occurred mass fluxes of gaseous and liquid moisture were following:

$$\left(D_{v,ef}\nabla\rho_v\right)_w = \mathbf{j}_{v,w} = 0 \quad (13)$$

$$\left(-K_l \nabla p_c\right)_w = \mathbf{j}_{l,w} = h_m\left(\frac{\rho_{v,w}}{\rho_{g,w}} - Y_{amb}\right) \quad (14)$$

These boundary conditions were valid when the liquid saturation was higher than the minimal saturation for water in the pendular form, i.e., $s > s_{min} = 0.25$. For the second period of drying when the liquid saturation dropped below minimum saturation (i.e., $s < s_{\min} = 0.25$) mass fluxes of gaseous and liquid moisture were following:

$$\left(-D_{v,ef}\nabla\rho_v\right)_w = \mathbf{j}_{v,w} = h_m\left(\frac{\rho_{v,w}}{\rho_{g,w}} - Y_{amb}\right) \quad (15)$$

$$\left(-K_l \nabla p_c\right)_w = \mathbf{j}_{l,w} = 0 \quad (16)$$

The thermal boundary condition for eq. (7) on the top wall was following:

$$\left(-k_{ef}\nabla T\right)_w = h_t\left(T_w - T_{amb}\right) + \Delta h_{lv}\mathbf{j}_{l,w} \quad (17)$$

where the last term on the right-hand side of eq. (17) referred to liquid moisture evaporation or condensation on the top wall.

Parameters of boundary conditions assumed during simulations were following: the temperature and relative humidity of drying air equal to $T_{amb} = 23.8$°C and $\varphi_{amb} = 44\%$, respectively, the heat transfer coefficient of $h_t = 22.5$ W/m^2/K and the mass transfer coefficient of $h_m = 0.0258$ kg/m^2/s. Initial conditions were following: the uniform brick temperature of $T_0 = 23.8$°C and uniform water saturation of $s_0 = 97\%$, which corresponded to the volumetric moisture content of $W_0 = 126.1$ kg/m^3.

3.2 Material properties and closing relationships

The relationships required to close systems of transport equations, eq. (1)-(2) and eq. (5)-(7), were the following [3]:

- Pores area per unit volume:

$$a_s = \frac{6}{d_{av}\left(1-\varepsilon_s\right)} \quad (18)$$

- Vapor diffusivity in pores:

$$D_{v,ef} = \frac{2.61\cdot10^{-5} M_v\left(1-\frac{W}{W_{cap}}\right)}{C_{dry}BT\left[0.503\left(1-\frac{W}{W_{cap}}\right)^2 + 0.497\right]} \quad (19)$$

- Effective thermal conductivity of the moist brick:

$$k_{ef} = k_s + 0.0047W \quad (20)$$

- Water permeability in the brick:

$$K_l = \frac{1.1437\cdot10^{-9}}{\left[1+\left(1.76\cdot10^{-5}\,p_c\right)^{4.3}\right]^{1.6}} \quad (21)$$

- Vapor saturation pressure:

$$p_{v,sat} = 614.3\exp\left(17.06\frac{T-273.15}{T-40.25}\right) \quad (22)$$

- Modified saturation pressure:

$$p^*_{v,sat} = p_{v,sat}\exp\left(-\frac{p_c M_v}{\rho_l BT}\right) \quad (23)$$

- Liquid saturation:

$$s = \frac{\varepsilon_l}{1-\varepsilon_s} \quad (24)$$

- Volumetric moisture content:

$$W = W_l + W_g = \rho_l\varepsilon_l + \rho_v\varepsilon_g \quad (25)$$

- Volumetric moisture content in the gaseous phase:

$$W_v = \frac{W/\rho_l - \varepsilon_p}{1/\rho_l - 1/\rho_v} \quad (26)$$

- Volumetric moisture content in the liquid phase:

$$W_l = \frac{\varepsilon_p - W/\rho_v}{1/\rho_l - 1/\rho_v} \quad (27)$$

- Retention curve which was applied to find the capillary pressure:

$$W(p_c) = \\ = W_{cap}\left\{\begin{array}{l} 0.846\left[1+\left(1.394\cdot 10^{-5}\,p_c\right)^4\right]^{-0.75} + \\ 0.154\left[1+\left(0.9011\cdot 10^{-5}\,p_c\right)^{1.69}\right]^{-0.408} \end{array}\right\} \quad (28)$$

- Water vapor density for saturation conditions:

$$\rho_{v,sat} = \frac{p^*_{v,sat} M_v}{BT} \quad (29)$$

- Effective heat capacity:

$$(\rho c)_{ef} = \varepsilon_s \rho_s c_s + \varepsilon_l \rho_l c_l + \varepsilon_g \rho_a c_{p,a} + \varepsilon_g \rho_v c_{p,v} \quad (30)$$

Moreover, the ideal gas relationship was used for calculations of dry and moist air as well as vapor parameters.

Simulations were carried out for the ceramic brick, which thermophysical properties are presented in Table 1.

3.3 Numerical implementation of models

3.3.1 Equilibrium model

The equilibrium model of heat and moisture transfer defined with eq. (1) and (2) was implemented in the framework of the in-house simulation software. The transport equations, eq. (1) and (2), were discretized on the 1D control volume mesh, based on the nodal representation. It meant that the nodes were also defined on boundaries of the domain, and two "half" control volumes were generated at both boundaries. The basic simulations were carried out for the uniform spatial mesh which had 30 elements across the domain. The transient terms in both equations were discretized with implicit Euler scheme and time step of 0.5 s was found to be enough to provide stable simulations. The idea of separated solver was utilized. It means that in each iteration the moisture transfer equation, eq. (1), was solved first and next, the supplementary material properties as well as volumetric moisture contents in gaseous and liquid phases were evaluated. On this basis the coefficients given by eq. (3) and the source term given by eq. (4) were updated. In the last step the energy balance equation, eq. (2), was solved.

3.3.2 Non-equilibrium model

The non-equilibrium model defined by eq. (5)-(7) was implemented in the commercial software ANSYS Fluent, which is based on the Finite Volume Method approach. Advanced customization interfaces, i.e., the User Define Function (UDF), User Define Scalar (UDS) and User Define Memory (UDM) were used during development of the numerical model. The computational model was constrained to two-dimensional (2D) geometry. Numerical simulations were conducted in the following way. For the considered case the model was configured to simulate 1D heat and moisture transfer in the ceramic brick. The basic mesh had 90 elements along the thickness of the brick, while 1 element was used along width of the brick. The time step size was equal to 0.25 s, which allowed to carry out stable simulations.

Table 1. Thermophysical properties assumed during simulations [13].

Property	Symbol and unit	Value
Universal gas constant	B (J/kmol/K)	8314
Dry air specific heat at constant pressure	$c_{p,a}$ (J/kg/K)	1005.0
Water specific heat	c_l (J/kg/K)	4192.1
Brick specific heat	c_s (J/kg/K)	840.0
Vapor specific heat at constant pressure	$c_{p,v}$ (J/kg/K)	1875.2
Water vapor resistance diffusion factor	C_{dry}	24.79
Average pore diameter	d_{av} (m)	$1.6\cdot10^{-5}$
Mass transfer coefficient between vapor and water in porous medium	h_{vl} (m/s)	10^{-4}
Brick thermal conductivity	k_s (W/m/K)	1.0
Dry air molecular mass	M_a (kg/kmol)	28.86
Vapor molecular mass	M_v (kg/kmol)	18.0
Capillary moisture content	W_{cap} (kg/m^3)	130.0
Volume fraction of pores (brick porosity)	ε_p	0.13
Latent heat of evaporation	Δh_{lv} (J/kg)	$2.5\cdot10^6$
Water density	ρ_l (kg/m^3)	1000.0
Brick density	ρ_s (kg/m^3)	2087.0

4 Results and discussion

Primarily, both proposed models were verified with the numerical data provided by Belleghem [14], which were obtained by applying the simplified equilibrium model. The temperatures inside the brick at 1 cm depth are compared in Fig. 2.

All simulations reflected the same initial and boundary conditions as well as material properties. Presented results show good conformity of temperature in the first stage of the process, and its similar duration. Both equilibrium models, considered in this paper and in [14] were expressed with the same parameters, namely W and T, but the one presented in [14] was simplified

and only the gradient in the capillary pressure was accounted for in the moisture transfer equation. It can explain differences in temperature in the second stage of drying predicted with these two equilibrium models. The results predicted by the non-equilibrium model also agreed well with predictions of both equilibrium models. Comparison of volumetric moisture content predicted with both considered models at the surface of the brick, and inside the building material, at 1 and 2 cm depth, reveals similar behaviour in corresponding points – see Fig. 3. At points located 1 and 2 cm from the dried surface moisture contents are very close. However, at the surface the considerable difference in the moisture content is observed in the second stage of the drying process. It is due to different levels of minimal saturation for water in the pendular form. In the non-equilibrium model this parameter was set to be equal to 25% of the capillary moisture content, but in the equilibrium model no specified minimal saturation was set.

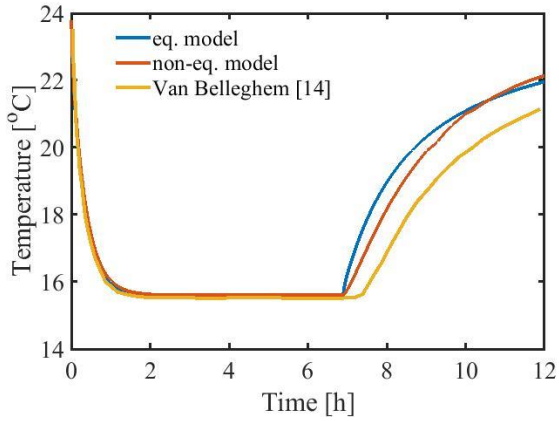

Fig. 2. Temporal variations of temperature in the brick at 1 cm depth predicted with equilibrium and non-equilibrium models, compared with reference data [14].

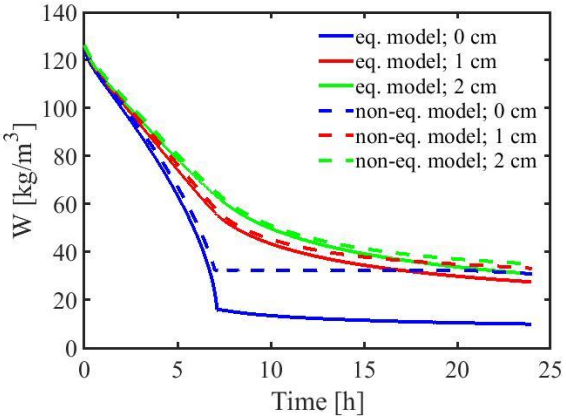

Fig. 3. Comparison of temporal variations of the volumetric moisture content predicted with equilibrium and non-equilibrium models, at the surface and inside the dried brick.

The total moisture contents in the wet brick, predicted with both considered models reveal similar behaviour but slightly diverged in time. The difference in moisture contents after 24 h does not exceed 5% of their initial values. It can be related to differences in formulations of models and presence in the non-equilibrium model of a-priori defined minimal saturation moisture content, enforcing change in the water transfer mode. Additionally, results predicted with the equilibrium model can be treated as the limiting values for the non-equilibrium models parametrized with h_{lv}. Therefore, the moisture content in the brick should be lower if predicted with equilibrium model.

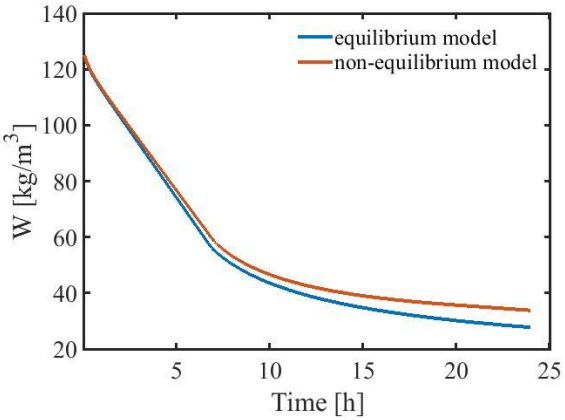

Fig. 4. Comparison of temporal variation of the total moisture content in the brick predicted with equilibrium and non-equilibrium models.

5 Conclusion

In this paper, the equilibrium and non-equilibrium simulation models of concurrent water moisture and heat transfer in the wet building material were developed and investigated. On the example of the simple, one dimensional drying problem of the uniform material both considered models are compared and their implementations are verified with the reference data [14]. Presented plots of temperature in the point inside the brick, at 1 cm depth, show good conformity in the first stage of drying. In the second stage some differences appear, but they can be related to slight differences between models, like enforced change in mode of moisture transfer in the non-equilibrium model. Differences are more pronounced, while compared variation of moisture content at the surface of the brick (Fig. 3) in the second stage of drying. The origin of this behaviour is similar as differences in temperature (Fig. 2), namely enforced change in mode of moisture transfer after the moisture content drops below the minimal saturation level. Differences in moisture content at the surface (Fig. 3) and total moisture content (Fig. 4) show that the equilibrium model predicts the limiting conditions for the moisture transfer, which can be attained when the parameter describing the rate of phase change between liquid and vapor phases in pores, h_{lv}, increases.

Comparison of various models of concurrent moisture and heat transfer shows differences between models. Their further development will be also related to their validation. It will be performed with experimental stands which are under development and testing and

which were described in recent publications [15] and [16].

This work was supported from European Union within the European Regional Development Fund under project no. POIR.04.01.02-00-0099/16 "Development of innovative technology of drying and moisture sealing of masonry walls, DryWall" granted by the National Centre for Research and Development (Poland).

References

1. M. Van Belleghem, L. De Backer, A. Janssens, M. De Paepe, *Proc. 9th International Conference on Heat Transfer, Fluid Mechanics and Thermodynamics, HEFAT2012*, 1095-1103 (2012)
2. M. Van Belleghem, M. Steeman, H. Janssen, A. Janssens, M. De Paepe, Build. Environ. **81**, 340-353 (2014)
3. H.-J. Steeman, M. Van Belleghem, A. Janssens, De M. Paepe, Build. Environ. **44**, 2176-2184 (2009)
4. M. Van Belleghem, H.-J. Steeman, M. Steeman, A. Janssens, M. De Paepe, Build. Environ. **45**, 2485-2496 (2010)
5. B. M. Janetti, L. P. M. Colombo, F. Ochs, W. Feist, Energy Build. **166** 550-560 (2018)
6. C. Belleudy, M. Woloszyn, M. Chhay, M. Cosnier, Int. J. Heat Mass Transf. **95**, 453-465 (2016)
7. R. Allam, N. Issaadi, R. Belarbi, M. El-Meligy, A. Altahrany, Heat Mass Transfer **54** 1579-1591 (2018)
8. P. Łapka, M. Wasik, P. Furmański, M. Seredyński, Ł. Cieślikiewicz, K. Pietrak, M. Kubiś, T.S. Wiśniewski, M. Jaworski, MATEC Web Conf. **240**, 01022 (2018)
9. M. Wasik, Ł. Cieślikiewicz, P. Łapka, P. Furmański, M. Kubiś, M. Seredyński, K. Pietrak, T.S. Wiśniewski, M. Jaworski, AIP Conf. Proc. **2078**, 020106 (2019)
10. X. Cheng, J. Fan, Int. J. Therm. Sci. **43**, 665-676 (2004)
11. P. Łapka, P. Furmański, Heat Mass Transfer **54**, 2461-2474 (2018)
12. P. Łapka, P. Furmański, T.S. Wiśniewski, Int. J. Numer. Methods Heat Fluid Flow **27**, 1078-1097 (2017)
13. M. Van Belleghem, B. Ameel, A. Janssens, M. De Paepe, *Proc. 8th International Conference on Heat Transfer, Fluid Mechanics and Thermodynamics, HEFAT2011*, 455-463 (2011)
14. M. Van Belleghem, *Modelling coupled heat and moisture transfer between air and porous materials for building applications*, PhD thesis, Ghent University, Belgium (2013)
15. Ł. Cieślikiewicz, P. Łapka, M. Wasik, M. Kubiś, K. Pietrak, T.S. Wiśniewski, P. Furmański, M. Seredyński, E3S Web Conf. **70**, 03003 (2018)
16. Ł. Cieślikiewicz, M. Wasik, M. Kubiś, P. Łapka, M. Bugaj, K. Pietrak, T.S. Wiśniewski, P. Furmański, M. Seredyński, Civ. Environ. Eng. Reports **29**, 53-65 (2019)